

## Universal Transition State for High-Pressure Zinc Blende to Rocksalt Phase Transitions

M. S. Miao and Walter R. L. Lambrecht

*Department of Physics, Case Western Reserve University, Cleveland, Ohio 44106-7079, USA*

(Received 25 January 2005; published 7 June 2005)

First-principles density functional calculations show that the high-pressure transitions of different semiconductors from zinc blende to rocksalt go through a transition state, which is universal in the sense that its position along the path and the corresponding geometry is independent of the chemical components of the semiconductor. This is explained using a Landau-like model expansion of the free energy in cosine functions of atomic position.

DOI: 10.1103/PhysRevLett.94.225501

PACS numbers: 61.50.Ah, 61.50.Ks, 62.50.+p, 64.70.Kb

The semiconductor phase transition from zinc blende (ZB) to rocksalt (RS) is one of the most intensively studied in high-pressure physics [1,2]. However, only recently, the direct observations of the transition mechanism became possible using picosecond time-resolved optical spectroscopy measurements for bulk materials [3] and by monitoring the shape changes for nanoparticles [4]. The time-resolved electron spectra indicated that the transformation must proceed through correlated atomic motions and that the system goes through a metastable intermediate state that has a long lifetime [5,6]. A path for the ZB to RS transition through an intermediate orthorhombic structure was proposed for SiC and ZnS [7] inspired by a molecular dynamic simulation [8].

We showed in our earlier work [9] that the transformation proceeds through a saddle-point-type transition state that has zero forces and zero stresses. It is then important to obtain the position and the structure of the transition state. This is usually a hard task since it requires a massive search in the multidimensional configuration space. However, for the ZB to RS transition, the transition state lies on Catti's path [7], which can be constructed by moving the atoms from their ZB positions to RS positions and letting the lattice relax. The orthorhombic path turns out to be very close to a slightly generalized monoclinic path, which was found to have the lowest transition barrier [10]. The relative position of the two sublattices  $z$  (or  $u = 0.5 - z$ ) is here used as an independent variable characterizing the transition path.

In this work, we used the above procedure to find the transition state (TS) of the ZB to RS transition for different semiconductor compounds, including II–VI, III–V, and group IV compounds. We found (1) the location and the geometry of the TS are identical for all the semiconductors investigated; (2) the lattice constants and the scaled volume (relative to the ZB volume) vary in a universal manner along the path for all the semiconductors; (3) the cosine function of the relative sublattice position can be used as an order parameter for expanding the enthalpy associated with the phase transition. The corresponding Landau-like phenomenological model clearly reveals that the position of

the TS does not depend on the chemical composition of the compounds.

The calculations are performed using Troullier-Martins pseudopotentials [11] and a plane wave basis. The Perdew-Wang generalized gradient approximation [12] is used for the exchange-correlation energy functional and potential. The energy cutoff is 80 Ry for systems containing Zn and N atoms and is 60 Ry for the others. We use  $8 \times 8 \times 8$   $k$  mesh for primitive cell calculations and  $4 \times 4 \times 4$   $k$  mesh for supercell calculations. The total energy converged to less than 1 meV/formula. Among the selected compounds [1,13,14], CdTe goes from ZB to the Cinnabar structure first before it becomes RS [15]. ZnTe transforms to Cinnabar and then to a  $Cmcm$  structure under high pressure [16]. InN is stable in the wurtzite structure at low pressure and transforms to RS under high pressure [17]. However, we choose these compounds for comparison reasons and study their hypothetical ZB to RS transition.

The transition pressures are obtained by comparing the enthalpy as the function volume dependence for ZB and RS structures. The transition barriers are then obtained for Catti's path under the transition pressure. The lattice constants are optimized to maintain the external pressure. The results are listed in Table I together with the ratios between the volumes of RS and ZB structures. The reduction of the volume from ZB to RS structures is about 20% for all compounds. The trends of the transition pressures with ionicity have been amply discussed in the literature [18,19].

The transition barriers are higher for III–V compounds than for II–VI compounds and is the highest for SiC. The changes of the enthalpy along the transition path are shown in Fig. 1 for CdS, ZnTe, InAs, and SiC. The enthalpy curves scaled to their barrier heights fall almost on a universal curve. Clearly, the peak, representing the TS, occurs at the same  $z \approx 0.34$  value for all cases. To obtain an accurate TS, we calculate more points around  $z = 0.35$  on Catti's path. The TS is determined when the forces are less than 1 mRy/a.u. As shown in Table I, the position of the TS is very close for all the semiconductors investigated in this work.

TABLE I. The transition pressure  $P_t$ , transition barrier  $\Delta H$ , volume for RS scaled to ZB  $V_{RS}/V_{ZB}$ , the position of the transition state  $z$  along the path, the  $a/b$  and  $c/b$  ratios for the transition state lattice, and the transition state volume scaled to ZB  $V_{TS}/V_{ZB}$ .

	$P_t$ (GPa)	$\Delta H$ (eV)	$V_{RS}/V_{ZB}$	$z$	$a/b$	$c/b$	$V_{TS}/V_{ZB}$
CdS	4.0	0.15	0.81	0.34	1.18	1.01	0.90
CdSe	3.6	0.15	0.81	0.34	1.19	1.01	0.91
CdTe	4.0	0.16	0.81	0.34	1.20	0.99	0.90
ZnS	14.5	0.19	0.84	0.34	1.19	1.01	0.92
ZnSe	12.5	0.18	0.84	0.34	1.20	1.00	0.92
ZnTe	9.25	0.23	0.83	0.34	1.20	1.01	0.92
InN	13	0.23	0.83	0.345	1.18	1.03	0.91
InP	8.5	0.32	0.82	0.335	1.18	1.02	0.91
InAs	6	0.31	0.82	0.34	1.20	1.06	0.91
SiC	63	0.73	0.81	0.34	1.20	1.04	0.91

The ratios of the optimized lattice constants for TS are also shown in Table I. The ratio  $a:b:c$  is around 1.2:1:1 for all the semiconductors. This indicates that the structure of the TS is universal for different semiconductors. Figure 2 shows the structure of the TS and the changes of the local bonding for ZB, TS, and RS states. We pick CdS as an example. The red spheres represent Cd atoms and the yellow ones S atoms. Clearly, ZB is tetrahedrally bonded. The bond length between the 4 S and the central Cd is 2.53 Å. The other 2 S atoms are farther away, about 4.85 Å. The S-S distance between the S atoms in the same tetrahedron is 7.81 Å, while the S-S distance in different tetrahedrons are 11.05 Å. In RS structure, all 6 S atoms form bonds with the central Cd atom and the bond length is 2.71 Å. The nearest neighbor S-S distance is also equal for all 6 S atoms, and is 7.24 Å. The bonding features of the TS

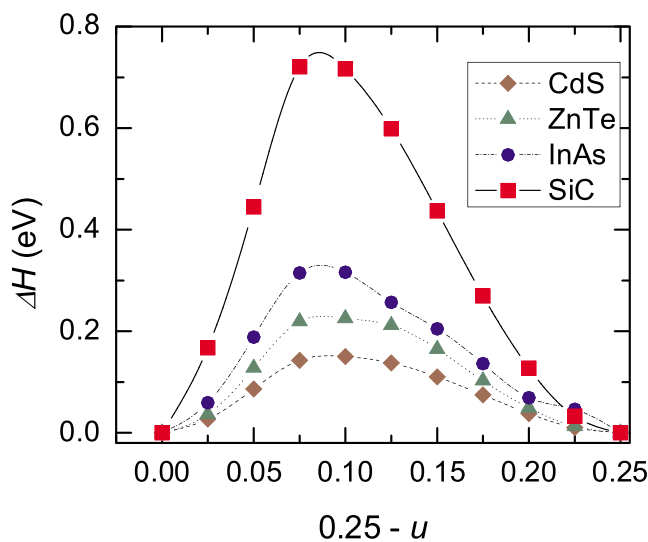


FIG. 1 (color online). The enthalpies for the structures along the orthorhombic ZB to RS transition path for CdS, ZnTe, InAs, and SiC. ZB is at  $u = 0.25$  and RS is at  $u = 0$ .

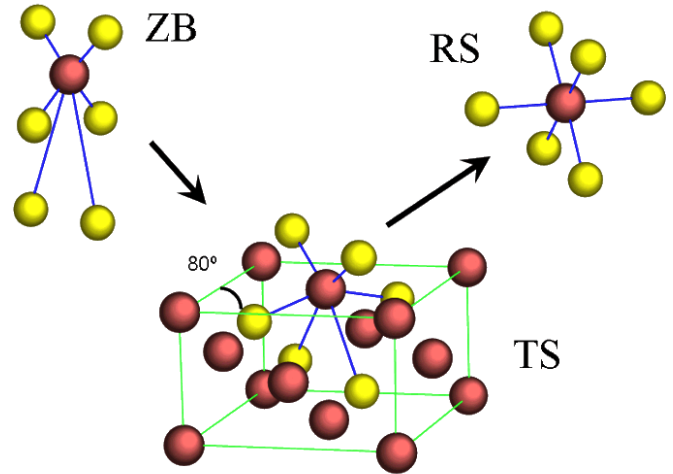


FIG. 2 (color online). The structure of the transition state and the local bonding changes from ZB to RS. The distorted fcc lattice is shown.

are between those of the ZB and the RS states. The bond length between the Cd and the four closest S are 2.54 and 2.60 Å, which is closer to the value of ZB state. However, the other 2 S atoms move much closer, and the distance is reduced to 3.46 Å. The 6 S atoms have three different distances, 3.88, 4.22, and 4.16 Å. During the transition, the angle between two faces of a cubic cell of the ZB state changes from 90° to 70.5° for the RS state. (See Fig. 6 in Ref. [8].) As shown in Fig. 2, this angle is about 80° for the TS state. The ratios of the volumes for TS and ZB can also be found in Table I. It shows that the reduction of the volume is ~10%, which is half of the reduction for the RS.

The shape of the cell also changes similarly for all the semiconductors along the transition path. The  $a/b$  and  $c/b$  ratios and the scaled volumes along the transition path are depicted for CdSe, ZnS, SiC, and InP in Fig. 3. The  $a/b$

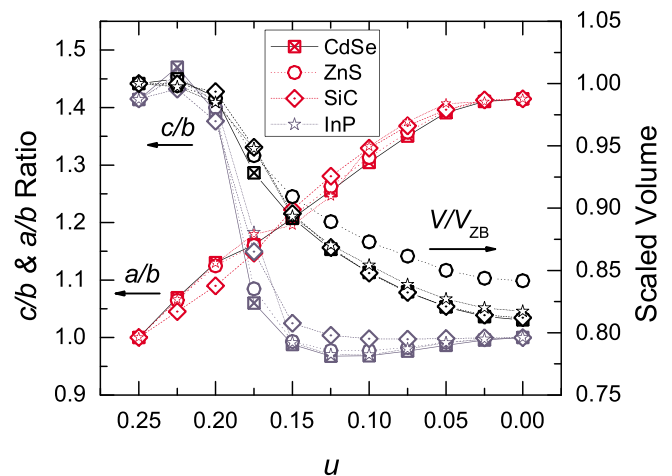


FIG. 3 (color online). The  $a/b$  and  $c/b$  ratios and the scaled volumes for the structures along the transition path for CdSe, ZnS, InP, and SiC.

and  $c/b$  ratio curves roughly overlap each other for various semiconductors. The  $a/b$  ratio and the  $c/b$  ratio behave differently along the transition path. The former changes almost linearly with the atomic position, except close to the RS state. On the other hand,  $c/a$  changes slowly near the ZB state and shows rapid changes near the TS. After the TS, it is almost flat and stays at the value of 1. The scaled volume also shows a “resistance” to the movement of the atoms near the ZB. After that it changes gradually to the RS value, faster around the TS and slower around the RS. The curves overlap with each other nicely, except for ZnS which has a slightly larger scaled volume for the RS state.

The ZB to RS transition is reconstructive, but the atom displacement during the transition is very large. As a result, the conventional phenomenological Landau model cannot be directly applied because it is hard to define an order parameter in this case. An alternative approach is to define the order parameter as a periodic function, of the atom displacement [20]. Obviously, this is valid only while the atom displacement stays periodic during the transition. Actually, many transitions satisfy this condition, including the  $\beta$ - $\omega$  transition, the bcc-hcp transition [21] and bcc-fcc transition that goes through the well known Bain path [22]. However, there are no numerical results showing the convergence of this Fourier expansion of the free energy.

The ZB to RS transition is more complicated than the above transitions. It can be characterized by two sets of movements, the atom displacement and the lattice relaxation. We calculated the total energy as a function of the atom displacement for systems with ZB and RS lattice vectors. The symbols in Fig. 4 show the results for CdS. The expansion of the energy in cosine functions of the

relative position of the two sublattices are shown as continuous lines in Fig. 4. The expansion is seen to converge very quickly and is different for different structures. For RS structure, it needs two cosine functions, while for ZB one cosine function is sufficient.

Another important feature of the ZB to RS transition is that the periodicity changes during the transition. For the ZB structure, the period for the  $u$  variable is 0.5 while for the RS structure it is 1. This feature is totally different from the other reconstructive transition, such as the  $\beta$ - $\omega$  transition, the bcp-hcp transition, and the bcc-fcc transition. The corresponding Landau model should include this feature. We calculated the energy as a function of atom displacement for the system with TS lattice vectors. The results for CdS are also presented in Fig. 4. This curve can be fitted by two cosine functions. This suggests it can be expressed as a linear combination of the energy functions for ZB and RS structures. Based on this result, we assume that the enthalpy of the system can be written as

$$H = \frac{1}{2}\eta^T \mathbf{C} \eta + A\eta^T \xi \cos 4\pi u + B(\eta^T \xi - \eta_Z^T \xi) \cos 2\pi u + D(\eta^T \xi - \eta_Z^T \xi) \cos 4\pi u - (A + B + D)\eta^T \xi, \quad (1)$$

in which  $\eta^T = (\eta_1, \eta_2, \eta_3)$  is the strain vector that contains only the diagonal elements of the strain tensor,  $\mathbf{C}$  is the elastic constants matrix in Voigt notation,  $\xi^T = (\xi_1, \xi_2, \xi_3)$  represents the vector character of the coupling between  $u$  and the strains, and  $A$ ,  $B$ , and  $D$  define the coupling strengths for each  $\cos 2\pi n u$  term in the Landau expansion. The model assumes that for each  $\cos 2\pi n u$  term the couplings to the different lattice vectors scale in the same way as specified by  $\xi$ . A constant shift is added to the stress so that the transition pressure becomes 0. For a more detailed discussion of this model with the special case  $D = 0$ , see Ref. [9].

The first order derivatives of the strains give the total stress in three directions of the orthorhombic cell and the derivative as a function of  $u$  gives forces on the atoms. At equilibrium, both stresses and forces should be zero,

$$\frac{\partial H}{\partial \eta^T} = \mathbf{C} \eta + A \xi \cos 4\pi u + B \xi \cos 2\pi u + D \xi \cos 4\pi u - (A + B + D) \xi = \mathbf{0}. \quad (2)$$

$$\frac{\partial H}{\partial u} = -4\pi A \eta^T \xi \sin 4\pi u - 2\pi B (\eta^T \xi - \eta_Z^T \xi) \times \sin 2\pi u - 4\pi D (\eta^T \xi - \eta_Z^T \xi) \sin 4\pi u = \mathbf{0}. \quad (3)$$

In the whole parameter space, only three points can have both zero stress and zero force. They are the initial ZB, the final RS, and the transition state. The ZB and RS are the minima, and the transition state is a saddle point. It is maximum along the steepest descent direction. Along Catti’s path, the stress is zero, but forces remain on the atoms. On the other hand, for the path with fixed strain and relaxed atom position, the forces are zero but stresses exist

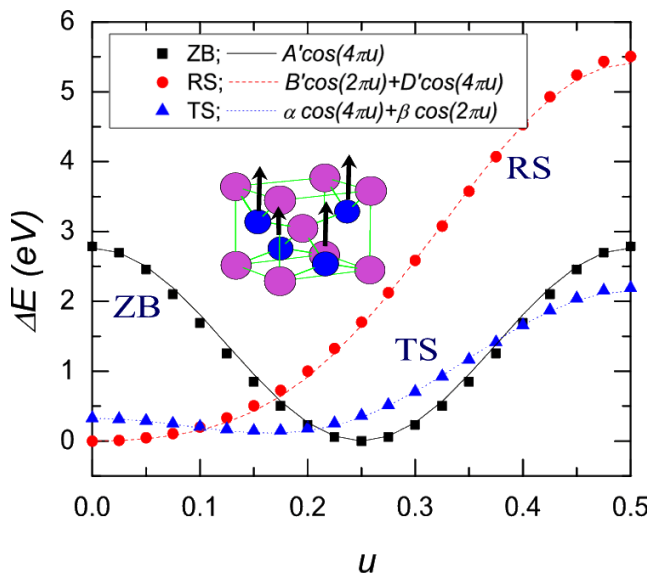


FIG. 4 (color online). The calculated and the fitted free energy dependence on the relative position of the sublattices for CdS. The arrows in the inset structure show the direction of motion corresponding to  $u$ . The primed parameters are the originals times  $\eta_Z^T \xi$ . For example,  $A' = A\eta_Z^T \xi$ .

TABLE II. The fitting parameters for the Landau model for ZB, RS, and TS structures.

	$A'$	$B'$	$D'$	$\alpha$	$\beta$	$z_{\text{mod}}$
CdS	1.382	-2.703	0.525	0.448	-0.909	0.35
CdSe	1.608	-2.905	0.594	0.497	-1.019	0.36
CdTe	1.763	-3.045	0.628	0.525	-1.114	0.36
ZnS	1.846	-2.505	0.512	0.545	-1.135	0.37
ZnSe	1.764	-3.075	0.621	0.568	-1.226	0.36
ZnTe	2.015	-3.125	0.594	0.610	-1.323	0.37
InN	1.811	-3.150	0.485	0.529	-1.142	0.36
InP	2.301	-3.707	0.639	0.734	-1.458	0.37
InAs	2.345	-3.700	0.682	0.831	-1.726	0.37
SiC	3.470	-5.255	0.708	1.081	-2.173	0.37

and are unequal along three directions, although the stress tensor is still traceless. However, both paths pass through the TS point [9].

By solving both equilibrium equations together, one can find the position of TS:

$$\cos 2\pi u = -\frac{3}{8} \frac{B}{A+D} + \frac{1}{8} \times \sqrt{\left(\frac{B}{A+D}\right)^2 + 32 \frac{AB}{(A+D)^2} + 64 \frac{A}{A+D}}. \quad (4)$$

By fitting the calculated energy function as shown in Fig. 4, one can obtain the parameters  $A' = A\eta_Z^T\xi$ ,  $B' = B\eta_Z^T\xi$ , and  $D' = D\eta_Z^T\xi$ . These parameters can be directly used in the above formula to calculate the position of the TS  $z_{\text{mod}}$ , as the extra  $\eta_Z^T\xi$  will cancel out. The results are listed in Table II. It clearly shows that the positions of the TS are very close for the different compounds and the values are close to the results obtained from the first-principles calculation, 0.34. This is because the TS does not depend on  $\xi$  explicitly and only on certain ratios of the parameters  $A$ ,  $B$ , and  $D$ , in fact, mostly on  $B/(A+D)$ . Furthermore, near the transition point the  $\cos^{-1}$  function varies slowly. Also shown in this table are the  $\alpha$  and  $\beta$  coefficients for the  $\cos 2\pi u$  and  $\cos 4\pi u$  expansions for the actual TS lattice when fitted directly to the first-principles results. When we determine the  $u$  value from the minimum of this curve, say the blue curve (triangles) in Fig. 4, we find  $z_{\text{fit}} = 0.34 \pm 0.005$  for all cases. This further demonstrates the internal consistency of our model.

In conclusion, we calculated the position and the geometry of the transition state along the transition path for the ZB to RS transition for different semiconductor compounds. We found that the TS is always at  $z = 0.34$  for all the semiconductors and the ratio of  $a:b:c$  is always close to 1.2:1:1. A Landau phenomenological model using cosine functions of the atom displacement as the order parameter is found to converge with one or two terms. Furthermore, the energy function between the ZB and the RS states is a superposition of the energy functions at the two end points.

The position of the transition state calculated from this model is found to be nearly independent of the parameters specific to the different compounds.

This work was supported by the Air Force Office of Scientific Research under Grant No. F49620-03-1-0010. Most of the calculations are performed on the AMD cluster at the Ohio Supercomputing Center and supported under Project No. PDS0145.

- [1] A. Mujica, A. Rubio, A. Muñoz, and R.J. Needs, *Rev. Mod. Phys.* **75**, 863 (2003).
- [2] J. Crain, G.J. Ackland, and S.J. Clark, *Rep. Prog. Phys.* **58**, 705 (1995); G.J. Ackland, *Rep. Prog. Phys.* **64**, 483 (2001).
- [3] M.D. Knudson and Y.M. Gupta, *Phys. Rev. Lett.* **81**, 2938 (1998); M.D. Knudson, Y.M. Gupta, and A.B. Kunz, *Phys. Rev. B* **59**, 11704 (1999); M.D. Knudson and Y.M. Gupta, *J. Appl. Phys.* **91**, 9561 (2002).
- [4] J.N. Wickham, A.B. Herhold, and A.P. Alivisatos, *Phys. Rev. Lett.* **84**, 923 (2000).
- [5] Z.P. Tang and Y.M. Gupta, *J. Appl. Phys.* **81**, 7203 (1997).
- [6] S.M. Sharma and Y.M. Gupta, *Phys. Rev. B* **58**, 5964 (1998).
- [7] M. Catti, *Phys. Rev. Lett.* **87**, 035504 (2001); *Phys. Rev. B* **65**, 224115 (2002).
- [8] F. Shimojo, I. Ebbsjö, R.K. Kalia, A. Nakano, J.P. Rino, and P. Vashishta, *Phys. Rev. Lett.* **84**, 3338 (2000).
- [9] M.S. Miao, M. Prikhodko, and W.R.L. Lambrecht, *Phys. Rev. Lett.* **88**, 189601 (2002); *Phys. Rev. B* **66**, 064107 (2002).
- [10] M.S. Miao and Walter R.L. Lambrecht, *Phys. Rev. B* **68**, 092103 (2003).
- [11] N. Troullier and J.L. Martins, *Phys. Rev. B* **43**, 1993 (1991).
- [12] J.P. Perdew and Y. Wang, *Phys. Rev. B* **45**, 13244 (1992).
- [13] A.L. Ruoff and T. Li, *Annu. Rev. Mater. Sci.* **25**, 249 (1995).
- [14] V. Ozoliņš and A. Zunger, *Phys. Rev. Lett.* **82**, 767 (1999).
- [15] M. Côté, O. Zakharov, A. Rubio, and M.L. Cohen, *Phys. Rev. B* **55**, 13025 (1997).
- [16] G.D. Lee and J. Ihm, *Phys. Rev. B* **53**, R7622 (1996).
- [17] N.E. Christensen and I. Gorczyca, *Phys. Rev. B* **50**, 4397 (1994).
- [18] J.R. Chelikowsky and J.K. Burdett, *Phys. Rev. Lett.* **56**, 961 (1986).
- [19] N.E. Christensen, S. Satpathy, and Z. Pawlowska, *Phys. Rev. B* **36**, 1032 (1987).
- [20] V.P. Dmitriev, S.B. Rochal, Yu.M. Gufan, and P. Toledano, *Phys. Rev. Lett.* **60**, 1958 (1988); P. Toledano and V. Dmitriev, *Reconstructive Phase Transitions in Crystals and Quasicrystals* (World Scientific Publishing, Singapore, 1996).
- [21] Z. Nishiyama, *Martensitic Transformations* (Academic Press, New York, 1978).
- [22] P. Alippi, P.M. Marcus, and M. Scheffler, *Phys. Rev. Lett.* **78**, 3892 (1997).